



ELSEVIER

Contents lists available at ScienceDirect

Ceramics International

journal homepage: [www.elsevier.com/locate/ceramint](http://www.elsevier.com/locate/ceramint)

# Tailorable magnetic properties of $\epsilon$ -Fe<sub>2</sub>O<sub>3</sub>/SiO<sub>2</sub> hybrid via alkaline etching

Yunguo Wang, Ji Ma, Sizhi Zuo-Jiang, Kezheng Chen\*

Lab of Functional and Biomedical Nanomaterials, College of Materials Science and Engineering, Qingdao University of Science and Technology, Qingdao 266042, China

## ARTICLE INFO

### Keywords:

Composites (B)  
Magnetic properties (C)  
Ferrites (D)  
SiO<sub>2</sub> (D)

## ABSTRACT

In this study, conventional silicon alkaline-etching procedure was utilized to tailor magnetic properties of  $\epsilon$ -Fe<sub>2</sub>O<sub>3</sub>/SiO<sub>2</sub> hybrid. It was found that the saturation magnetization, coercivity and exchange bias field can be readily changed and tailored by altering the etching time and frequency in a set of sodium hydroxide solutions. The relative quantity of  $\epsilon$ -Fe<sub>2</sub>O<sub>3</sub> phase, the proximity or pinning effect derived from SiO<sub>2</sub> phase as well as the phase transformation from  $\epsilon$ -Fe<sub>2</sub>O<sub>3</sub> to  $\alpha$ -Fe<sub>2</sub>O<sub>3</sub> during etching treatment were three main factors to its controllable magnetic properties. This work will shed new light on the development of functional  $\epsilon$ -Fe<sub>2</sub>O<sub>3</sub>/SiO<sub>2</sub> composites with tailorable magnetism in practical magnetically-relevant applications.

## 1. Introduction

Development of high-performance magnetic materials with desirable and controllable magnetic properties is highly demanded for magnetic recording and magnetic resonance imaging. During the last decade or so, many of these research activities [1–7] were devoted to singular synthetic routes for magnetic materials with tailorable magnetic properties. As a result, a substantial amount of information is now available on crystallography, structural chemistry, magnetic ordering, proximity effect, and other new properties [8–12] that make materials have an enormous technological impact in the new generation of ultra-high density magnetic information storage devices, magnetic sensors, refrigerant materials and permanent magnets [13–17]. Compared to the above topical areas, nonetheless, much less attention has been paid to their magnetism controls after fabrication, although it has been well conceived that suchlike robust and facile post-treatment can enhance stability and reproducibility of the final product.

$\epsilon$ -Fe<sub>2</sub>O<sub>3</sub>, a polymorph of iron oxide, features the merits of giant coercive field ( $H_c$ ) as large as 20 kOe at room temperature, coupled magnetoelectric properties, and ferromagnetic resonance capability [18–23], whereas its pure phase can be hardly synthesized due to the presence of silicon phase [24–26] that imposes space restriction and serves to limit the size of  $\epsilon$ -Fe<sub>2</sub>O<sub>3</sub> nanoparticles [8,24]. In this work, we tailor-make various  $\epsilon$ -Fe<sub>2</sub>O<sub>3</sub>/SiO<sub>2</sub> nanosystems with controllable ferromagnetism by alkaline-etching silicon after fabrication. This synthetic route is not only highly feasible, cost-effective and reproducible, but also enables new insights into the fundamental understanding of the related magnetic effects in  $\epsilon$ -Fe<sub>2</sub>O<sub>3</sub> phase.

## 2. Experimental

### 2.1. Syntheses of $\epsilon$ -Fe<sub>2</sub>O<sub>3</sub>/SiO<sub>2</sub> hybrids

All chemicals were analytical grade and used as received without further purification. In a typical experimental procedure [27], 2.9 mmol of Fe(NO<sub>3</sub>)<sub>3</sub>·9H<sub>2</sub>O and 0.18 mmol of Ba(NO<sub>3</sub>)<sub>2</sub> were dissolved into 30 mL of water, while 7 mL of ammonia was dissolved into 23 mL of water. These two solutions were mixed together with vigorous stirring before 7 mL of tetraethyl orthosilicate (TEOS) being injected. After stirring for another 12 h, the light yellow precipitate was separated by centrifugation, washed successively with distilled water and absolute ethanol, and finally calcined at 1100 °C in the air for 4 h to form brown products.

In order to modify the ferromagnetism of the resultant product, a set of sodium hydroxide solutions (1 mol/L) were utilized to etch silicon phase for 3, 6, 12, 24, 36, 72 and 120 h. On the other hand, with the total etching time of 72 h held constant, the raw product was etched by 1 mol/L of NaOH solution for 1, 2, 3, 4, and 6 times with time intervals of 72, 36, 24, 18 and 12 h, respectively. After each time interval, NaOH solution was renewed and its concentration was maintained at 1 mol/L prior to the following etching procedure. All these dark red precipitates were separated by centrifugation, washed successively with distilled water and absolute ethanol, and finally dried in the vacuum at 60 °C for 4 h.

### 2.2. Characterization

The XRD patterns were recorded on a powder X-ray diffractometer

\* Corresponding author.

E-mail address: [kchen@qust.edu.cn](mailto:kchen@qust.edu.cn) (K. Chen).

<http://dx.doi.org/10.1016/j.ceramint.2017.09.031>

Received 15 July 2017; Received in revised form 29 August 2017; Accepted 4 September 2017  
0272-8842/ © 2017 Elsevier Ltd and Techna Group S.r.l. All rights reserved.

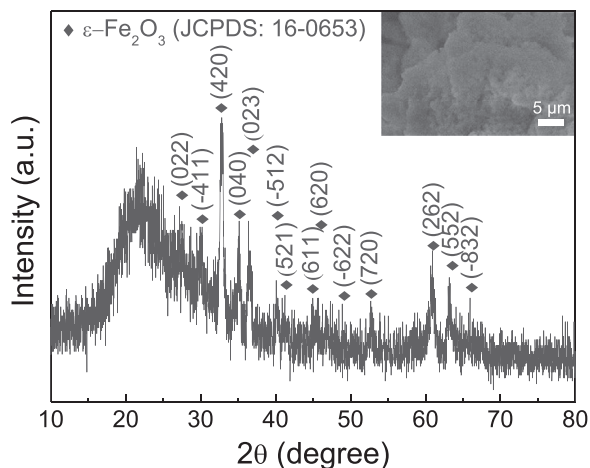


Fig. 1. XRD pattern of the as-synthesized  $\epsilon$ -Fe<sub>2</sub>O<sub>3</sub>/SiO<sub>2</sub> hybrid product. The typical SEM image is shown as an inset.

(Rigaku D/max-rA) equipped with a rotating anode and a Cu K $\alpha$ 1 radiation source ( $\lambda = 1.5406 \text{ \AA}$ ) at a step width of  $0.02^\circ$ . Field emission scanning electron microscope (FE-SEM) images were collected on a JEOL JSM-6700F FE-SEM. Fe<sup>3+</sup> ion concentrations were determined by inductively coupled plasma-optical emission spectrometry (ICP-OES, Perkin-Elmer Optima 8000). Magnetic measurements were carried out using a commercial superconducting quantum interference device magnetometer (SQUID MPMS-XL5, U.S.A.).

### 3. Results and discussion

The chemical composition of the as-synthesized product is shown in Fig. 1, in which the diffraction peaks at  $27.50^\circ$ ,  $30.20^\circ$ ,  $32.94^\circ$ ,  $35.14^\circ$ ,  $36.40^\circ$ ,  $40.08^\circ$ ,  $41.24^\circ$ ,  $45.58^\circ$ ,  $45.74^\circ$ ,  $48.90^\circ$ ,  $52.72^\circ$ ,  $60.96^\circ$ ,  $63.16^\circ$ ,  $65.94^\circ$  can be unambiguously indexed to (022), ( $\bar{4}11$ ), (420), (040), (023), ( $\bar{5}12$ ), (521), (611), (620), ( $\bar{6}22$ ), (720), (262), (552), ( $\bar{8}32$ ) of monoclinic structure  $\epsilon$ -Fe<sub>2</sub>O<sub>3</sub> (JCPDS PDF No. 16–0653), respectively. Besides, a hump located around  $22^\circ$  demonstrates the presence of amorphous silicon in the product. The morphology of the  $\epsilon$ -Fe<sub>2</sub>O<sub>3</sub>/SiO<sub>2</sub> hybrid is shown in the inset of Fig. 1, from which it mainly composes of heavily aggregated  $\epsilon$ -Fe<sub>2</sub>O<sub>3</sub> nanoparticles dispersed in flocculent SiO<sub>2</sub> matrix. Its microstructure is clearly presented by the low- and high-magnified TEM images in Fig. 2, from which iron oxide nanoparticles with an average diameter of ca. 10 nm are dispersively distributed in the amorphous silica matrix.

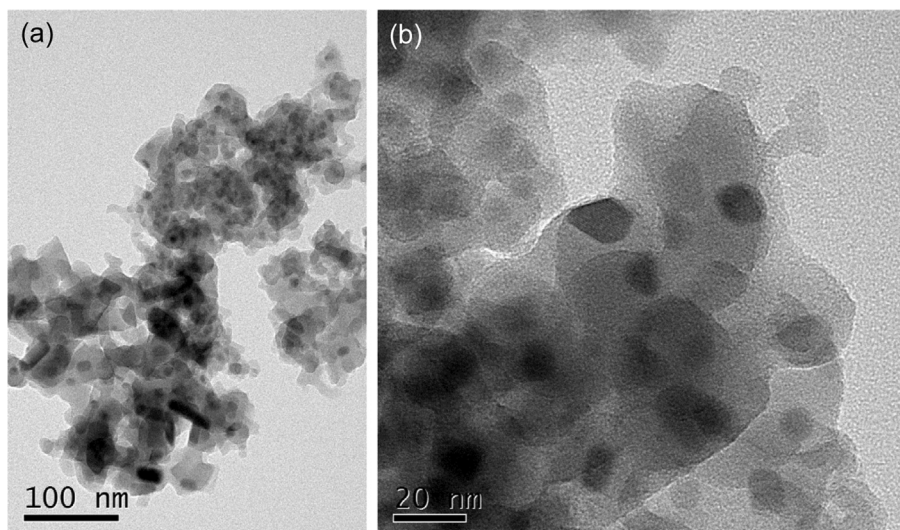


Fig. 2. TEM images of the as-synthesized  $\epsilon$ -Fe<sub>2</sub>O<sub>3</sub>/SiO<sub>2</sub> hybrid product with (a) low- and (b) high- magnifications.

After alkaline-etching this pristine  $\epsilon$ -Fe<sub>2</sub>O<sub>3</sub>/SiO<sub>2</sub> product for various time, the flocculent SiO<sub>2</sub> matrix is getting inconspicuous (Fig. 3) due to the reaction of  $\text{SiO}_2 + 2\text{NaOH} \rightarrow \text{Na}_2\text{SiO}_3 + \text{H}_2\text{O}$  to yield soluble sodium silicate. In stark contrast, the boundaries of  $\epsilon$ -Fe<sub>2</sub>O<sub>3</sub> nanoparticles are becoming distinct and well-defined because of the relatively inert nature of  $\epsilon$ -Fe<sub>2</sub>O<sub>3</sub> phase in alkaline aqueous solution.

Fig. 4a is XRD patterns of etched products for different time. In general, diffraction peaks at  $27.40^\circ \sim 27.62^\circ$ ,  $29.72^\circ \sim 30.02^\circ$ ,  $32.70^\circ \sim 32.98^\circ$ ,  $34.86^\circ \sim 35.14^\circ$ ,  $36.40^\circ \sim 36.72^\circ$ ,  $39.90^\circ \sim 40.20^\circ$ ,  $41.36^\circ \sim 41.48^\circ$ ,  $45.22^\circ \sim 45.58^\circ$ ,  $45.66^\circ \sim 45.86^\circ$ ,  $48.86^\circ \sim 48.98^\circ$ ,  $52.46^\circ \sim 52.84^\circ$ ,  $60.70^\circ \sim 60.88^\circ$ ,  $63.00^\circ \sim 63.18^\circ$ ,  $65.74^\circ \sim 66.04^\circ$  can be assigned to (022), ( $\bar{4}11$ ), (420), (040), (023), ( $\bar{5}12$ ), (521), (611), (620), ( $\bar{6}22$ ), (720), (262), (552), ( $\bar{8}32$ ) of monoclinic structure  $\epsilon$ -Fe<sub>2</sub>O<sub>3</sub> (JCPDS PDF No. 16–0653), respectively. Notably, the intensity of diffraction peak of amorphous silicon around  $22^\circ$  was nearly unchanged in the initial etching stage, while it significantly decreases as prolonging the etching time beyond 12 h. The magnetic hysteresis loops of these products measured at room temperature are shown in Fig. 4b, in which the saturation magnetization ( $M_S$ ) is virtually unchanged when the etching time is below 12 h. Further increasing etching time to 72 h, the  $M_S$  value monotonically increases to 8.7 emu/g, which is 3.6 times as large as that below 12 h. This  $M_S$  increment can be ascribed to the ever-decreasing amount of silicon phase during alkaline etching procedure. As prolonging the etching time to 120 h, the  $M_S$  value is almost unchanged and located around 9 emu/g, indicating complete consumption of sodium hydroxide etching agent after 72 h. It is noteworthy that all magnetic hysteresis loops in Fig. 4b exhibit a sudden magnetization falloff near the origin, which has also been observed in many previous literatures due to the presence of weak ferromagnetic  $\alpha$ -Fe<sub>2</sub>O<sub>3</sub> and non-ferromagnetic SiO<sub>2</sub> phases [19,26].

The presence of SiO<sub>2</sub> has profound effect on coercive fields ( $H_c$ ) at different etching time. Fig. 5a shows all etched products exhibit large  $H_c$  values ( $> 12.5 \text{ kOe}$ ) and they increase as prolonging the etching time to 36 h. This variation tendency of coercivity bears striking similarities with that of weight percent of Fe<sub>2</sub>O<sub>3</sub> as observed in Fig. 5b. The weight percent of Fe<sub>2</sub>O<sub>3</sub> is estimated on the basis of Fe<sup>3+</sup> ion concentration. Typically, 10 mg of etched products were separately dispersed in 70 mL of hydrochloric acid aqueous solutions (12 wt%) and sonicated for 5 days. Then the concentrations of iron ions in supernatant (marked as C) were determined by ICP-OES. The weight percent of Fe<sub>2</sub>O<sub>3</sub> (denoted as  $W_{\text{Fe}_2\text{O}_3}$ ) is given by

$$W_{\text{Fe}_2\text{O}_3} = \frac{C \times 70(\text{mL}) \times M_{\text{Fe}_2\text{O}_3}}{2 \times M_{\text{Fe}} \times 10(\text{mg})} \times 100\% \quad (1)$$

here  $M_{\text{Fe}}$  and  $M_{\text{Fe}_2\text{O}_3}$  denote the molar mass of iron and Fe<sub>2</sub>O<sub>3</sub>,

Download English Version:

<https://daneshyari.com/en/article/5437288>

Download Persian Version:

<https://daneshyari.com/article/5437288>

[Daneshyari.com](https://daneshyari.com)